Received: 14 March 2018 | Revised: 13 August 2018 | Accepted: 14 August 2018

DOI: 10.1002/cnm.3145

RESEARCH ARTICLE - APPLICATION

WILEY

A comparative study of porous medium CFD models for flow diverter stents: Advantages and shortcomings

Nicolás Dazeo | Javier Dottori | Gustavo Boroni | Ignacio Larrabide

Pladema - CONICET, Universidad Nacional del Centro de la Provincia de Buenos Aires, Buenos Aires, Argentina

Correspondence
Nicolás Dazeo, Pladema - CONICET, Universidad Nacional del Centro de la Provincia de Buenos Aires, Buenos Aires, Argentina.
Email: ndazeo@exa.unicen.edu.ar

Present Address
Pladema, Pinto 399, Tandil, Buenos Aires, Argentina

Funding information
Consejo Nacional de Investigaciones CientÍficas y Técnicas; Fondo para la Investigación CientÍfica y Tecnológica, Grant/Award Number: PICT 2016-0116 and PICT Start-up 2015-0006; Nvidia

Abstract

In computational fluid dynamics, there is a high interest in modeling flow diverter stents as porous media due to its reduced computational loads. One of the main difficulties of such models is proper parameter setup. Most authors assume flow diverter's wire screen as an isotropic and homogeneous medium, while others proposes anisotropic configurations, yet very little is discussed about the effect of these assumptions on model's accuracy. In this paper, we compare the effect of different models on hemodynamics in relation to their parameters. The fidelity and efficiency of the different models to capture wire screen effect on fluid flow are quantitatively analyzed and compared.

KEYWORDS

CFD, flow diverter, modeling, porous medium

1 | INTRODUCTION

Flow diverter (FD) stents are endovascular devices used to treat intracraneal aneurysms. They are placed in the parent vessel of an aneurysm to divert the flow from the aneurysm sac.[1,2] Computational fluid dynamics (CFD) has been largely used to predict the behavior and assess changes in local blood flow when a FD is placed on the parent vessel.[3-5] The default way for modeling stent wires is as no-slip boundaries inside the fluid domain.

Flow diverter permeability and porosity are the main features driving their ability to modify local flow.[6] Because of this, it seems natural to model such devices using porous medium (PM) models. In the case of braided FD, porosity is determined not only by the FDs design but also by the final positioning of the FD mesh inside the vessel. Flow patterns show significant sensitivity to PM parameters; therefore, determination should be well taken care.[7] Different PM models have been proposed in the literature in the recent years. Augsburger et al[8] compared the simulation of two intracranial aneurysm with a full FD model and a PM model. This approach requires a previous simulation of the FD with a no-slip boundaries model in an isolated simulation to determine PM parameters. Karmonik et al[9] demonstrate that a PM model with arbitrary parameters of a FD presents a decrease in velocities and wall shear stress at the aneurysm sac. Morales and Bonnefous obtain PM parameters from FD properties, independent of the deployment.[10] Raschi et al[11] applied a numerical correlation estimated by Idelchik[12] for parameter estimation. Ohta et al[13] placed an FD parallel to the flow in different rectangular test sections. Results show that the test section significantly affects pressure drop on parallel direction.

Abbreviations: CFD, computational fluid dynamics; FD, flow diverter; DNS, direct numerical system; PM, porous medium.

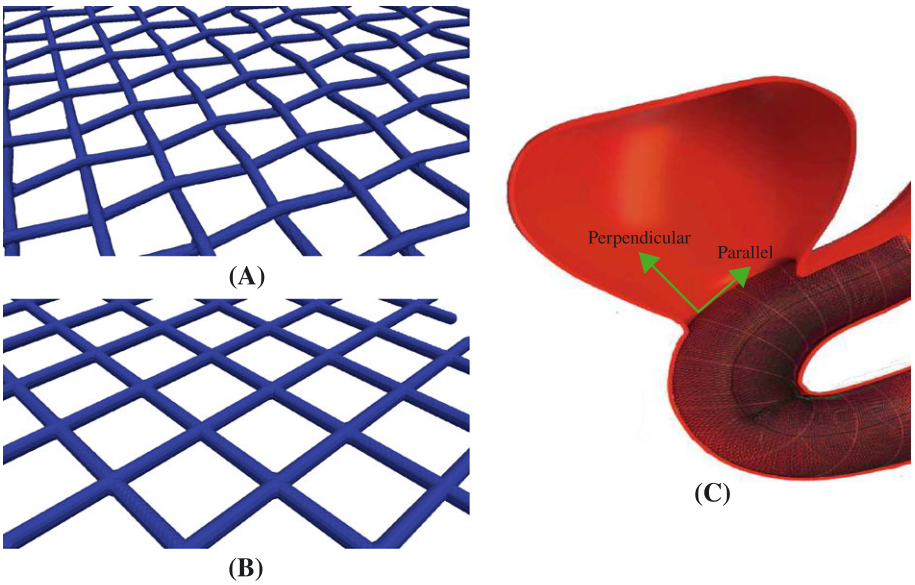

FIGURE 1 A, Entangled wire model, B, simplified wire model, and C, flow diverter stent deployed on a vessel with a sidewall aneurysm

In this work, numerical simulations of the hemodynamics in ideal geometries were performed for no-slip boundaries models and PM models in literature reproducing typical intracranial flow conditions. Stents are modeled as flat wire screens in a square section pipe. We investigate the dependency of different model variables for different sections and flow scenarios. In particular, FD segments placed in the simulations were perpendicular and parallel to the flow direction. In addition, wires are deployed with different angles due to the changes in the diameter and direction of a stent in the flow domain. Also, two types of wire-crossing models are considered: a more realistic model defined as entangled wire model (EWM) (Figure 1A) and simplified model defined as a simplified wire model (SWM) (Figure 1B) usually applied in literature.

The placement of an FD on the parent vessel results in a decrease in the mean flow velocity in the aneurysm. Flow interacts both parallel and perpendicular to the braided mesh (Figure 1C). The degree of flow reduction and distribution through the neck depends on the configuration of the stent. On the other hand, in a single-stent cell, a change in the direction (cell width) due to a change in the diameter of the stent produces a corresponding change in the longitudinal direction (cell height) to keep the wire length constant, resulting in a change in the cell internal angles.[14]

2 | MATERIALS AND METHODS

Porous models in literature are implemented for different configurations. A total of 90 different configurations were considered: 45 where the flow direction was perpendicular to the wire screen and 45 parallel to it. Models were tested in idealized geometries (channels) resembling dimensions and fluid conditions typically found when modelling of intracranial aneurysms. The corresponding modifications of hemodynamic variables such as average velocity and pressure drop were measured and assessed. In the following, we describe the technical considerations assumed during the different experiments.

2.1 | FD geometry

The braided mesh of an FD can vary between models and manufacturers. In this study, we assessed an average case, with wires of $t = 5 \times 10^{-5}$ m thickness threads crossing each other and separated by $l = 3.12 \times 10^{-4}$ m (Figure 2). The braided mesh is represented as a flat, infinitely large, wire screen. The PM thickness was chosen to be the same as the FD wires thickness, ie, 5×10^{-5} m.

A PM can be mathematically modeled with two terms, representing viscosity and inertia, for each spatial dimension. To measure resistance in each direction, the screen was placed at the center of the channel, both perpendicular and parallel to the flow. Both configurations can be seen in Figure 3A,B.

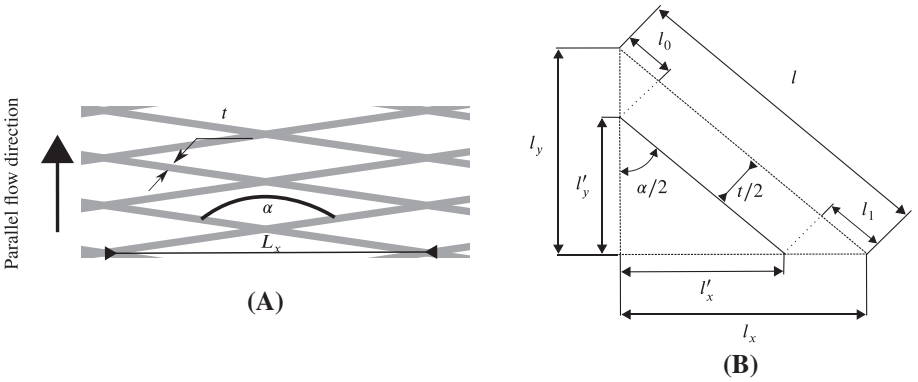

FIGURE 2 A, Configuration of flattened braided mesh. B, Derivated configuration values for a wire section

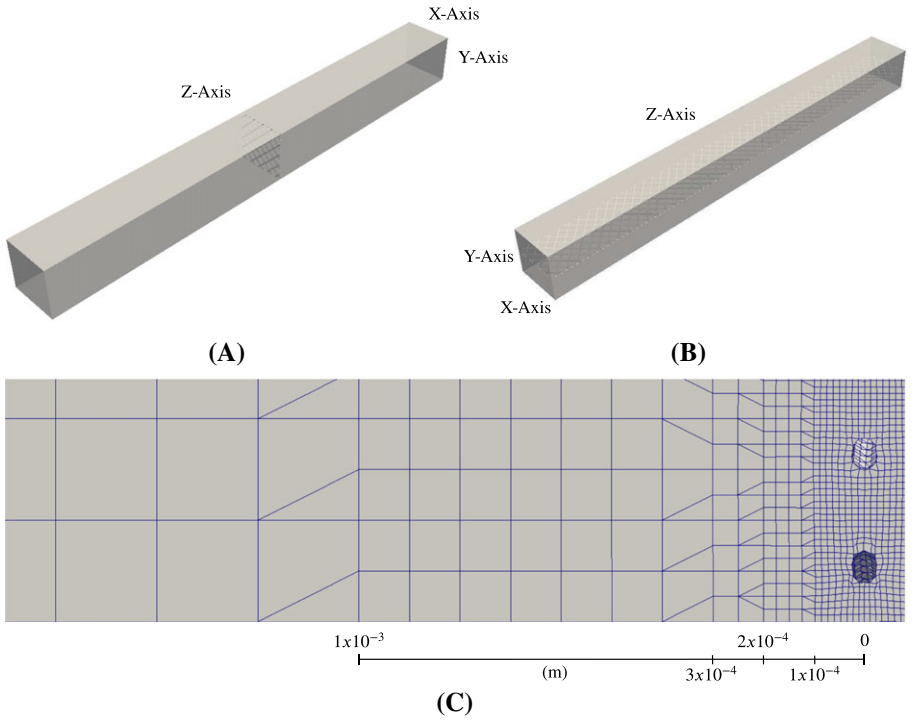

FIGURE 3 0.2 m long, 0.02m × 0.02m section channels. Both A, perpendicular and B, parallel configuration and C, cell division of channel near to the flow diverter

In a real geometry, FD internal angles depend both FD design, local anatomy of the treated vessel and deployment technique. Simulations were run for angles varying from 30° to 150° in 15° steps. Table 1 depicts porosity and pore density for each angle. Extreme angles were ignored as they imply a total obstruction of the flow. For the case of flow perpendicular to the screen, simulations are symmetric over 90° because the flow direction is perpendicular to the axial plane of the stent (where α is measured). On the other hand, in the cases where the flow is parallel to the screen (the direction of flow in relation to the angle α is indicated in Figure 3A), the simulations do not behave symmetric with respect to 90°.

2.2 | Channel geometry

A straight channel 0.2 m long, with a 0.02m × 0.02m cross section, with a single inlet and a single outlet, was considered. The spatial discretization was performed starting from regular polyhedral elements of 2×10^{-4} m a side. The grid was refined incrementally with the distance to the wire screen at 1×10^{-4}, 2×10^{-4}, 3×10^{-4}, and 1×10^{-3} m (Figure 3C). For the no-slip boundaries models, cell faces where snapped to the wire surface producing a mesh compliant to the shape of the stent wires.

TABLE 1 Number of pores per square meter and porosity by angle

α, °	Pore density, $1/m^2$	Porosity, %
30	64901392.06	0.501686463
45	40241270.35	0.6653459046
60	31132096.62	0.7266602493
75	27246436.98	0.7531065421
90	26132767.8	0.7607318854
105	27246436.98	0.7531065421
120	31132096.62	0.7266602493
135	40241270.35	0.6653459046
150	64901392.06	0.501686463

TABLE 2 Properties of analyzed PM models[a]

Model	Darcy coefficient	Forchheimer coefficient	Anisotropic	Required simulations
Idelchik[12]	$\frac{11\mu}{d_h \Delta L}$	$\frac{\rho}{2\Delta L}\left(1.3\,(1-\beta)+\left(\frac{1}{\beta}-1\right)^2\right)$	No	0
Raschi et al[11]	$\frac{8.8\mu}{d_h \Delta L}$	$\frac{0.86\rho}{2\Delta L}\left(1.3\,(1-\beta)+\left(\frac{1}{\beta}-1\right)^2\right)$	No	0
Augsburger et al[8]	Fitted from simulations		Yes	10
Morales et al[16]	$\frac{2\mu\pi^2(1-\epsilon)^2}{\epsilon^3\phi^2}$	$\frac{\sqrt{2}\rho 1.2\pi(1-\epsilon)}{\epsilon^2\phi}$	No	0

[a]The first column shows the analyzed PM models. The second and third columns contain the equations to calculate Darcy and Forchheimer coefficients. The fourth column states if the method can create an anisotropic PM. The fifth column contains required simulations to get coefficients.

2.3 | Simulation setup

Numerical experiments were performed to quantitatively compare different PM models. For this purpose, the open source finite volume software OpenFOAM was used.[15] OpenFOAM offers multiple solvers to compute Navier-Stokes (N-S) equations. In this case, steady-state computational simulations were used in all the experiments.

Morales et al[16] state that local differences between Newtonian and non-Newtonian fluids in coiled intracranial aneurysm are not sufficient to alter the main flow. With this in mind, and because velocities in aneurysms treated with coils are smaller than velocities in aneurysms treated with FDs, blood behavior can be safely assumed as Newtonian in the former. Kinematic viscosity was considered as $\nu = 3.774 \times 10^{-06} \mathrm{m}^2/\mathrm{s}$ to match with human blood.

Flow rate was fixed at the inlet, and a pressure equal to 0 was set at the outlet. Wire surface was set as a no-slip boundary. Slip boundary condition was chosen for the remaining boundaries (top, bottom, and lateral walls of the channel). Then the only source of flow resistance remained to be the wire screen.

Average velocity in a cerebral vessel usually treated with FDs are in the order of 0.1 m/s. [17,18] To recreate normal physiological fluctuations, different flow rates were imposed at the channel: 0.025, 0.05, 0.1, 0.2, and 0.4 m/s.

2.4 | PM model assessed

Flow diverter geometries described in Section 2.1 were modeled using different PM models described in literature. A brief description for each model is presented in Table 2. Homogeneous medium was considered for the different models.

2.4.1 | Idelchik (1986)

Idelchik studied hydraulic resistance of wire screens for multiple shapes and sizes.[12] This was evaluated for geometries, much larger than those of FD stents. For the case of rhomboidal structures, the following equations are proposed:

$$d = \frac{11\mu}{d_h \Delta L}, \tag{1}$$

$$f = \frac{\rho}{2\Delta L}\left(1.3\,(1-\beta) + \left(\frac{1}{\beta} - 1\right)^2\right), \tag{2}$$

where d_h is the hydraulic diameter, defined as the ratio of four times the void volume V_{void} to the wetted surface area A_w:

$$\begin{aligned} d_h &= \frac{4V_{void}}{A_w} \\ &= \frac{4l_x\, l_y\, r - 2\pi r^2\left(l + \frac{1}{2}l_0 + \frac{1}{2}l_1\right)}{\pi r\left(l + \frac{1}{2}l_0 + \frac{1}{2}l_1\right)} \\ &= \frac{4l_x\, l_y}{\pi\left(l + \frac{1}{2}l_0 + \frac{1}{2}l_1\right)} - 2r, \end{aligned} \tag{3}$$

and β is the cross-sectional porosity, defined as the open area A_{open} by the total area A_{total}:

$$\beta = \frac{A_{open}}{A_{total}} = \frac{l'_x l'_y}{l_x\, l_y}. \tag{4}$$

2.4.2 | Raschi et al (2014)

Raschi et al evaluates Idelchik model through a comparison with an immerse boundary simulation used as ground truth.[11,19] The authors state that an overprediction of Δp in the immerse boundary approach is observed in Idelchik model, and they propose a correction with two fitting parameters: Darcy correction (c_D) and Forchheimer correction (c_F),

$$\Delta P = c_d d + c_f f. \tag{5}$$

They found an overprediction for Darcy of $25 \pm 3\%$ and Forchheimer $16 \pm 3\%$, and they propose $c_d = 0.75$, $c_f = 0.86$. Following algebraic, we find

$$c_d d \cdot 1.25 = d \tag{6}$$

$$c_d \cdot 1.25 = 1 \tag{7}$$

$$c_d = \frac{1}{1.25} = 0.8, \tag{8}$$

which was used in our experiments. Different correction factors as indicated in Raschi et al[11] were also tested. Results from Equation 8 where chosen as these produced the best results in our experiments.

2.4.3 | Augsburger et al (2011)

Augsburguer et al proposed modeling an FD stent as a PM in Augsburger et al.[8] The media was modeled by addition of a viscous and an inertial loss to the momentum fluid equations. These terms contribute to the pressure gradient across the porous cells.

The FD is modeled as a homogeneous anisotropic PM. This implementation requires a coefficient for each new term in each orthogonal direction. In their work, the authors obtain those coefficients via SWM simulations.

Simulations are done in a pipe of 1.128×10^{-3} m in diameter for perpendicular flow and a 0.9×10^{-3} m per 0.2×10^{-3} m rectangular parallelepiped for parallel flow. The wire screen is then introduced in the sections, as shown on Figure 4 with a no-slip boundary condition. A relation between velocity and pressure drop is then computed:

$$\Delta P = d \cdot U + f \cdot U^2, \tag{9}$$

where U is the velocity vector, d is the viscous or Darcy term, and f is the inertial or Forchheimer term.

The authors do not provide details about lateral boundaries, and channel length is not specified. In this work, 2×10^{-3} m and 0.2×10^{-3} m are chosen for perpendicular and parallel flows, respectively, and slip conditions for walls.

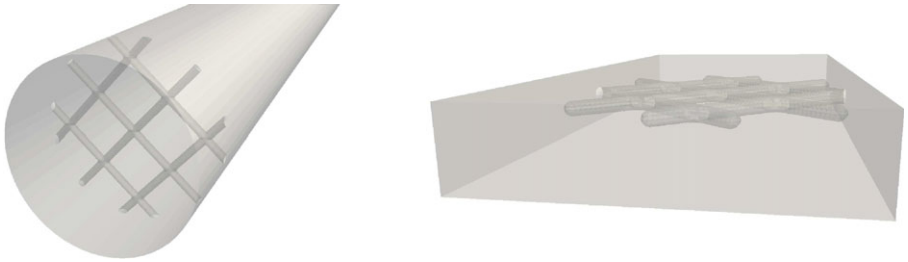

(A) **(B)**

FIGURE 4 A, Perpendicular and B, parallel placement of the stent in the test volumes

2.4.4 | Morales et al (2014)

Morales et al proposed an analytical model for PM coefficients.[10] Darcy and Fochheimer values calculated in this model are invariant on the deployment. The model describes porous coefficients as

$$d = \frac{\mu}{k}, \tag{10}$$

$$f = \frac{\rho C_d}{\sqrt{k}}, \tag{11}$$

where μ and ρ are the dynamic viscosity and density of the fluid, respectively. C_d is drag coefficient factor, set to $C_d = 1.2$ by the author. k is the permeability, obtained from

$$k = \frac{\epsilon^3}{cS^2}, \tag{12}$$

where ϵ is the average porosity, c is fixed to 2 for cylinders, and

$$S = \frac{\pi(1-\epsilon)}{\phi}, \tag{13}$$

with ϕ strut thickness.

For experiments in this paper, we obtain the average porosity considering each angle evaluated: from 15° to 165°, in 15° steps.

2.5 | Mesh convergence

An extra level of refinement was tested to assess discretization size. The simulation was ran for the highest velocity, on a 90° wire crossing FD. Both pressure drop and velocity profile were measured. The pressure drop rendered a relative error of

$$\frac{|\Delta P - \Delta P_{extra\_refined}|}{\Delta P_{extra\_refined}} = 0.34\%. \tag{14}$$

Velocity profile relative mean squared error was less than $2.1 \times 10^{-4}\%$ between the most refined mesh and the previous one.

2.6 | Porous media coefficients

Porous media coefficients were calculated for each model. On perpendicular configuration, values are symmetric at 90°. Higher values are found at the extreme angles 30° and 150°, decreasing closer to 90°. Augsburger et al model is the only nonisotropic model, with the lowest value on parallel configuration, between 105° and 120°.

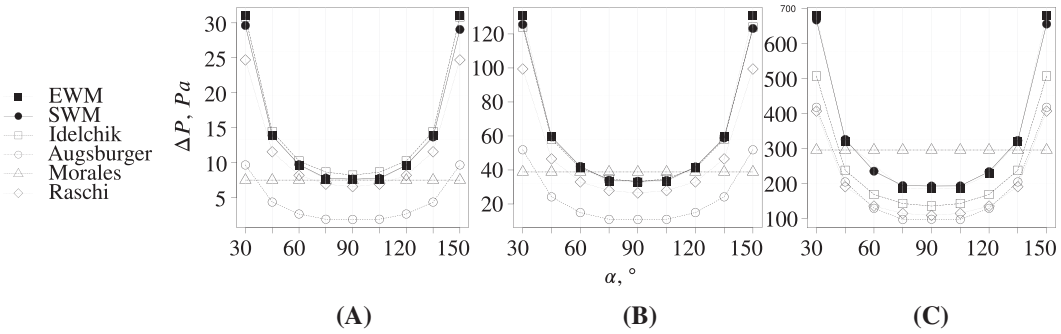

FIGURE 5 Pressure drop vs flow diverter mesh α angle for each model. Inlet velocity was set to A, 0.025, B, 0.1, and C, 0.4 m/s. EWM, entangled wire model; SWM, simplified wire model

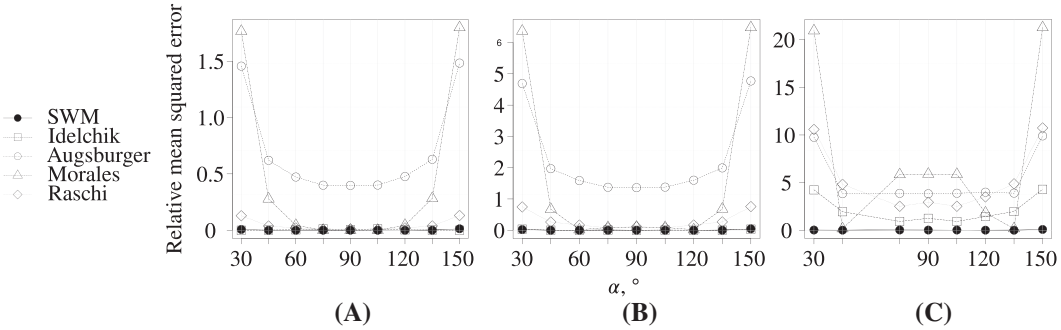

FIGURE 6 Relative pressure drop squared error vs α angle in degrees for each model. Inlet velocity is set as A, 0.025, B, 0.1, and C, 0.4 m/s. SWM, simplified wire model

3 | RESULTS

On perpendicular flow, the wire screen creates a pressure drop between the inlet and the outlet. Pressure is measured on both sides and the difference is calculated.

Ohta et al state that, on parallel configuration, pressure drop is not representative of the medium: The influence of the channel geometry has much more influence in pressure than the wire screen.[13] We therefore compare the shape of the velocity profile and the average velocity in the PM between models to assess which one provides a better approximation.

3.1 | Perpendicular flow analysis

Pressure drops for each angle and for each model were calculated. Figure 5 shows pressure drops by angle for three velocities. The EWM simulations shows a higher resistance at the extreme angles 30° and 150° , decreasing closer to 90°. Simplified wire model has a good agreement with EWM. Idelchik model produces the pressure drop that is closer to EWM, overestimating it at low velocities ($v < 0.1$) and underestimating it at higher ones ($v > 0.1$). Raschi model underestimates pressure drop more than Idelchik. Augsburger model underestimates pressure drop proportionally irrespective of velocity. Morales model sets a constant resistance for all angles.

The relative squared error between each PM model, SWM, and EWM (Figure 6) was computed, and it was observed that it increases with higher velocity, showing the worst performance near extreme angle of the braided mesh. Between 45° and 135°, average SWM mean squared error is of 0.5%. With a 0.4 m/s velocity, there is also a small decrease in precision in models near 90°.

3.2 | Parallel flow analysis

For parallel flow configuration, velocity profiles were studied. In Figure 7A, no-slip boundaries models and PM models profiles' for same angle and inlet velocity are shown. In a qualitative assessment, we observe that velocity profiles were similar between models.

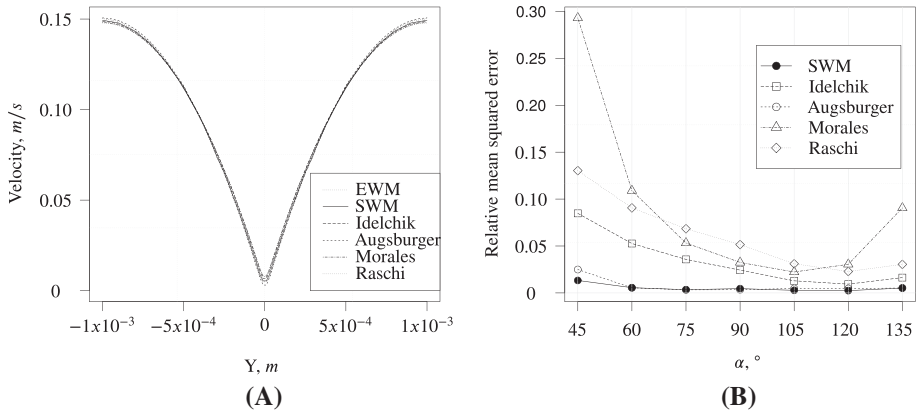

FIGURE 7 A, Velocity profiles on a 90° parallel screen across Y-axis for each model. A velocity of 0.1 m/s is set on the inlet boundary. B, Relative mean squared error vs α angle for each porous medium model. EWM, entangled wire model; SWM, simplified wire model

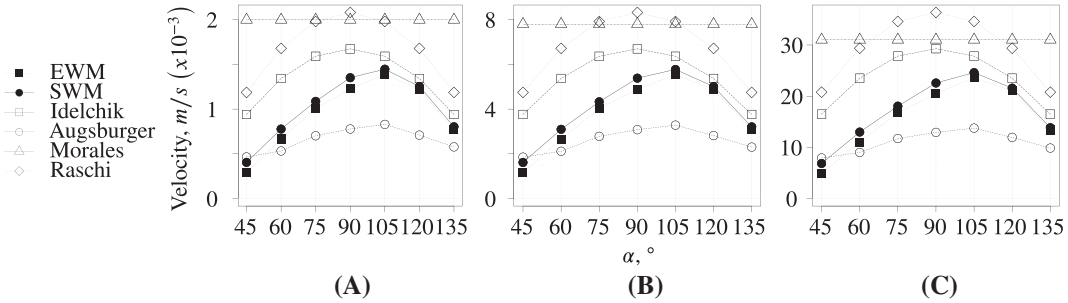

FIGURE 8 Average velocity at the porous zone vs α angle for each porous model. Inlet velocity is set to A, 0.025, B, 0.1, and C, 0.4 m/s. EWM, entangled wire model; SWM, simplified wire model

Velocity boundaries between the free flow and the porous media were analyzed at the selected velocities (Figure 8). It must be remarked that velocity is not symmetric between complementary angles. Entangled wire model simulation shows the highest velocity for the braided mesh configuration at 105°. Simplified wire model shows a very small difference with EWM. On Idelchik model, velocity is faster than expected, with a better approximation at higher angles. Augsburger produced lower velocities than DNS on the medium, having the highest velocity at 105° and lower velocities on the extremes. In Morales model, velocity is independent of the braided mesh angle. In Raschi model, there are higher velocities than Augsburger, both with the maximum at 90°.

Porous medium velocity profiles were compared with EWM (Figure 7B). Simplified wire model shows a small relative mean squared error of less than 0.013. Augsburger model is the PM that presented the lowest relative mean squared error in angles below 90° . Idelchik model fits better on angles from 90° to 150°. Morales model got the best approximation at 105°, always with a larger error than Augsburger and Idelchik. Raschi error has its maximum of 0.5% at 30°, decreasing to a minimum of 0.1% at 150°. Morales model has the largest relative error, with a value of 0.13% at 45°, and its best is assessed by Raschi at 150° of 0.01%.

4 | DISCUSSION

Flow diverter stents modify local flows by their permeability and inertial resistance. This features are based on the FD design parameters such as strut thickness and distance in between them. After deployment in the patient, the local geometry is modified locally by its final configuration. When the braided mesh is curved or compressed at the inner side of a curve, the angle between struts changes, reducing the free space producing heterogeneous porosity.

Difference between EWM and SWM is negligible (pressure drop, approximately 0.5%; velocity, approximately 0.013). Previous research[20,21] modeled FD stents in realistic geometries considering entangled wires. From our results, we conclude that differences are minimal with regard to pressure drop.

There are many PM models for FD in the literature, but a comparison between them was not performed yet. In the present study, we analyzed the influence of FD on parallel and perpendicular flows. Intermediate dispositions can be safely interpolated as presented on previous studies.[22,23] Similar results were obtained for no-slip boundaries models and different PM models. Porous medium coefficients for same configuration have a small variation between models. Their values are in the same orders of magnitude. Nevertheless, flow differences were significant, in accordance with Li et al. [7]

First, Idelchik model for generic wire screens is a good approximation for perpendicular flow. The model does not account for parallel flow, using the same values as in the perpendicular case, becoming an isotropic medium. As this model depends on local properties of the braided mesh, it requires knowing final configurations of the stent. However, this property allows a heterogeneous medium implementation. This method allows creating an isotropic but heterogeneous PM from a known FD configuration and a few equations. Raschi et al propose to use Idelchik model plus a correction factor specific to FD. Nevertheless, error values on Raschi models are bigger than Idelchik, which leads the authors to interpret that the correction factor might be inverted, as presented in Raschi et al.[11] Inverted factors were tested without improvements. Correction factor may depend on specific geometry; in this case, no-slip boundaries model simulations could not be avoided. Anyway, the correction factor could reduce the number of simulations required, due to the fact that Idelchik model reproduce perpendicular flow velocity shape across angles and proposed correction maintain that shape. Ausburger model coefficients are based on no-slip boundaries simulation results, which are different for each FD model deployed on each patient geometry. This entails that a different CFD simulation is prepared for each patient to obtain the porous model parameters. Then the simulations show different results for complementary angles. For this reason, Augsburger coefficients are rendered asymmetric with respect to 90° angles. Therefore, this model can approximate the shape of both perpendicular (Figure 6) and parallel (Figure 8) curves. On the other hand, it requires no-slip boundaries model simulations for coefficient estimations for each stent being modeled, which entails great computational time and model preparation for each stent. Also, in the case of parallel coefficients, they are biased by the shape and size of the test channel. If a heterogenous media is intended, braided mesh geometry must be divided, and each sample simulated independently. Nevertheless, this method requires as input the 3D geometry of a placed FD, so it can be applied on any type of stent. Computational cost must be considered, as this method could be as computationally expensive as no-slip boundaries model or more.

Morales model is independent of wire configuration, and only mean porosity is required. Coefficient values are constant irrespective of wire configuration (angle and separation); hence, only one calculation is needed for each stent being modeled. On the other hand, as coefficients are constant and do not change with the wire crossing angle, this method will provide a lower accuracy if used for realistic deployment analysis nor on heterogeneous media. This method is ideal when a first approximation of the FD is desired, without knowledge of stent configuration, and at a low computational cost.

Most methods disregard the effect of specific parallel coefficients of PM models and assume the model as isotropic. On the studied models, only Augsburger proposes a mean for measuring parallel PM parameters based on pressure drop. According to Ohta et al,[13] it is not a proper way to evaluate the parallel configuration of a braided mesh. Furthermore, our results shows that the three components, ie, the perpendicular and each parallel component, should have different parameters. In parallel configuration, resistance is higher in the direction of the smaller angle. This difference may be due to the alignment of braided wires with flow direction. On the basis of this observation, we propose to use velocity profiles to measure effectiveness of PM models in parallel configurations. Future methods may use this metric to determine each of the parallel PM coefficients.

Nevertheless, some limitations in our study must be remarked. First, this article studies stents behavior on ideal geometries. Due to the CFD analysis design, the influence of the channel on the flow is negligible, and all hemodynamic effects are attributable to the FD mesh. Second, the FD geometry used is a generic one, not representing any particular device available in the market. The result changes when design variables are changed that can be approached with the same methodology. Still, adjusting the corresponding geometrical parameters to those of one particular stent should result in a representative model for it. Also, the comparison method can be applied to others; hence, similar results are expected. Finally, simulations are stationary, with constant inlet velocities. Stationary simulations are good approximations on laminar flow regimes.[24] However, pulsatile flow could entail inertia effects, which might deserve a study on their own.

5 | CONCLUSIONS

In the present work, we quantitatively studied different methods to represent an EWM FD stent with a reduced computational load. Difference between EWM and SWM is negligible compared with the difference between EWM and PM models. The isotopic PM models are a good approximation, but they can be improved with anisotropic models. Morales model does not need much information about the deployed configuration of the stent, making it ideal for a first approximation of the results. Idelchik equations can be used to obtain perpendicular porosity coefficients for wire screens. Pressure drop in Augsburger simulation based method is affected by the channel shape; a velocity profile–based method may provide more accurate values.

ACKNOWLEDGMENTS

This project is partly funded by PICT Start-up 2015-0006 and PICT 2016-0116 - FONCYT - ANPCYT of Argentina. N.D. is supported by CONICET PhD grant. The Titan Xp used for this research was donated by the NVIDIA Corporation. The financial support of these institutions is greatly appreciated.

ORCID

Nicolás Dazeo http://orcid.org/0000-0002-0563-6732

REFERENCES

1. Sadasivan CR, Cesar L, Seong J, et al. An original flow diversion device for the treatment of intracranial aneurysms: evaluation in the rabbit elastase-induced model. *Stroke; J Cereb Circ*. March 2009;40(3):952-8.
2. Ma D, Dargush GF, Natarajan SK, Levy EI, Siddiqui AH, Meng H. Computer modeling of deployment and mechanical expansion of neurovascular flow diverter in patient-specific intracranial aneurysms. *J Biomech*. July 2012;45(13):1-8.
3. Mut F, Raschi M, Scrivano En, et al. Association between hemodynamic conditions and occlusion times after flow diversion in cerebral aneurysms. *J Neurointerv Surg*. April 2015;7(4):286-290.
4. Larrabide I, Aguilar ML, Morales HG, et al. Intra-aneurysmal pressure and flow changes induced by flow diverters: relation to aneurysm size and shape. *Am J Neuroradiol*. 2013;34(4):816-822.
5. Larrabide I, Kim M, Augsburger L, Villa-Uriol MC, Rüfenacht DA, Frangi AF. Fast virtual deployment of self-expandable stents: method and in vitro evaluation for intracranial aneurysmal stenting. *Med Image Anal*. 2012;16(3):721-730.
6. Kim M, Taulbee DB, Tremmel M, Meng H. Comparison of two stents in modifying cerebral aneurysm hemodynamics. *Ann Biomed Eng*. 2008;36(5):726-741.
7. Li Y, Zhang M, Verrelli DI, et al. Sensitivity study on modelling a flow-diverting stent as a porous medium using computational fluid dynamics. In: Engineering in Medicine and Biology Society (EMBC), 2017 39th Annual International Conference of the IEEE. IEEE; 2017:3389-3392.
8. Augsburger L, Reymond P, Rufenacht DA, Stergiopulos N. Intracranial stents being modeled as a porous medium: flow simulation in stented cerebral aneurysms. *Ann Biomed Eng*. 2011;39(2):850-863.
9. Karmonik C, Chintalapani G, Redel T, et al. Hemodynamics at the ostium of cerebral aneurysms with relation to post-treatment changes by a virtual flow diverter: a computational fluid dynamics study. In: Conference Proceedings : … Annual International Conference of the IEEE Engineering in Medicine and Biology Society. Osaka, Japan: IEEE Engineering in Medicine and Biology Society. Annual Conference, 2013:1895-1898.
10. Morales H, Bonnefous O. Modeling hemodynamics after flow diverter with a porous medium. Beijing, China: In: IEEE; 2014:1324-1327.
11. Raschi M, Mut F, Löhner R, Cebral JR. Strategy for modeling flow diverters in cerebral aneurysms as a porous medium. *In J Numer Methods Biomed Eng*. 2014;30(9):909-925.
12. Idelchik IE, Fried E. *Handbook of Hydraulic Resistance*. New York, NY: Hemisphere Publishing; 1986.
13. Ohta M, Anzai H, Miura Y, Nakayama T. Parametric study of porous media as substitutes for flow-diverter stent. *Biomat Biomech Bioeng*. 2015;2(2):111-125.
14. Mut F, Cebral JR. Effects of flow-diverting device oversizing on hemodynamics alteration in cerebral aneurysms. *Am J Neuroradiol*. 2012;33(10):2010-2016.
15. Jasak H, Jemcov A, Tukovic Z. Openfoam: A C++ library for complex physics simulations. In: International Wworkshop on Coupled Methods in Numerical Dynamics, Vol. 1000 IUC; 2007; Dubrovnik, Croatia:1-20.
16. Morales HG, Larrabide I, Geers AJ, Aguilar ML, Frangi AF. Newtonian and non-Newtonian blood flow in coiled cerebral aneurysms. *J Biomech*. 2013;46(13):2158-2164.
17. Ford MD, Alperin N, Lee SH, Holdsworth DW, Steinman DA. Characterization of volumetric flow rate waveforms in the normal internal carotid and vertebral arteries. *Physiol Meas*. 2005;26(4):477.

18. Cebral JR, Castro MA, Putman CM, Alperin N. Flow-area relationship in internal carotid and vertebral arteries. *Physiol Meas*. 2008;29(5):585-594.
19. Raschi MA. Computational modeling of flow diverting devices in intracranial aneurysms; 2013.
20. Flórez-Valencia L, Serrano ED, Reyes JR, et al. Virtual deployment of pipeline flow diverters in cerebral vessels with aneurysms to understand thrombosis. Nice, France: In: MICCAI-STENT'12 The 1st International MICCAI-Workshop on Computer Assisted Stenting; 2012:49.
21. Ma D, Dargush GF, Natarajan SK, Levy EI, Siddiqui AH, Meng H. Computer modeling of deployment and mechanical expansion of neurovascular flow diverter in patient-specific intracranial aneurysms. *J Biomech*. 2012;45(13):2256-2263.
22. Bear Jacob. *Dynamics of Fluids in Porous Media*. New York: Courier Corporation; 2013.
23. Castagnino WA. Modelos útiles en el manejo de los acuíferos reales. In: CEPIS; 1984:129-99.
24. Geers AJ, Larrabide I, Morales HG, Frangi AF. Approximating hemodynamics of cerebral aneurysms with steady flow simulations. *J Biochem*. 2014;47(1):178-185.

How to cite this article: Dazeo N, Dottori J, Boroni G, Larrabide I. A comparative study of porous medium CFD models for flow diverter stents: Advantages and shortcomings. *Int J Numer Meth Biomed Eng*. 2018;e3145. https://doi.org/10.1002/cnm.3145